Supplementary Materials

Interplay between Fe(II) and Fe(III) and Its Impact on Thermoelectric Properties of Iron-Substituted Colusites $Cu_{26-x}Fe_xV_2Sn_6S_{32}$

Alexey O. Polevik [1], Alexey V. Sobolev [1], Iana S. Glazkova [1,2], Igor A. Presniakov [1], Valeriy Yu. Verchenko [1,3], Joosep Link [3], Raivo Stern [3] and Andrei V. Shevelkov [1,*]

[1] Department of Chemistry, Lomonosov Moscow State University, 119991 Moscow, Russia; a.o.polevik@mail.ru (A.O.P.); alex@radio.chem.msu.ru (A.V.S.); janglaz@bk.ru (I.S.G.); ipresniakov1969@mail.ru (I.A.P.)
[2] Department of Chemistry, MSU-BIT University, Shenzhen 517182, China
[3] National Institute of Chemical Physics and Biophysics, 12618 Tallinn, Estonia; jooseplink@gmail.com (J.L.); raivo.stern@gmail.com (R.S.)
* Correspondence: shev@inorg.chem.msu.ru

Table of Contents

Table S1. Atomic parameters in the crystal structures of $Cu_{26-x}Fe_xV_2Sn_6S_{32}$.

$Cu_{25}Fe_1V_2Sn_6S_{32}$						
Atom	**Site**	***x***	***y***	***z***	**Occ.**	U_{iso}
Cu1/Fe1	6*d*	0.25	0	0.5	0.8333/0.1667 [a)]	0.0075(7)
Cu2	8*e*	0.2471(1)	0.2471(1)	0.2471(1)	1	0.0084(6)
Cu3	12*f*	0.2533(1)	0	0	1	0.0066(4)
V1/Sn2	2*a*	0	0	0	0.80(1)/0.20	0.002(1)
Sn1	6*c*	0.25	0.5	0	0.71(6) [b)]	0.0021(1)
Sn11	24*i*	0.243(1)	0.505(1)	0.006(1)	0.073(16)	0.005(1)
S1	8*e*	0.1255(3)	0.1255(3)	0.1255(3)	1	0.002(4)
S2	24*i*	0.3761(1)	0.3665(1)	0.1257(1)	1	0.0006(1)
$Cu_{22}Fe_2V_2Sn_6S_{32}$						
Atom	Site	*x*	*y*	*z*	Occ.	U_{iso}
Cu1/Fe1	6*d*	0.25	0	0.5	0.667/0.333 [a)]	0.0138(10)
Cu2	8*e*	0.2507(7)	0.2507(7)	0.2507(7)	1	0.0219(9)
Cu3/V2	12*f*	0.2516(3)	0	0	0.94(1)/0.06	0.0146(7)
V1	2*a*	0	0	0	1	0.008(3)
Sn1	6*c*	0.25	0.5	0	1	0.0110(5)
S1	8*e*	0.1205(6)	0.1205(6)	0.1205(6)	1	0.006(4)
S2	24*i*	0.3773(4)	0.3679(4)	0.1277(6)	1	0.0120(18)
$Cu_{23}Fe_3V_2Sn_6S_{32}$						
Atom	Site	*x*	*y*	*z*	Occ.	U_{iso}

Cu1/Fe1	6*d*	0.25	0	0.5	0.42(3)/0.58	0.0143(8)
Cu2	8*e*	0.2482(4)	0.2482(4)	0.2482(4)	1	0.0205(6)
Cu3/V2	12*f*	0.2519(2)	0	0	0.95(1)/0.05	0.0127(4)
V1/Cu4	2*a*	0	0	0	0.92(1)/0.08	0.0141(6)
Sn1	6*c*	0.25	0.5	0	1	0.0141(2)
S1	8*e*	0.1243(6)	0.1243(6)	0.1243(6)	1	0.040(3)
S2	24*i*	0.3778(3)	0.3686(3)	0.1251(4)	1	0.0033(5)
			$Cu_{22}Fe_4V_2Sn_6S_{32}$			
Atom	Site	*x*	*y*	*z*	Occ.	U_{iso}
Cu1/Fe1	6*d*	0.25	0	0.5	0.34(3)/0.66	0.0144(3)
Cu2	8*e*	0.2527(3)	0.2527(3)	0.2527(3)	1	0.0144(3)
Cu3/V2	12*f*	0.2515(3)	0	0	0.95(2)/0.05	0.0144(3)
V1/Cu4	2*a*	0	0	0	0.73(5)/0.27	0.008(2)
Sn1	6*c*	0.25	0.5	0	1	0.0077(4)
S1	8*e*	0.1238(8)	0.1238(8)	0.1238(8)	1	0.021(6)
S2	24*i*	0.3758(3)	0.3690(3)	0.1270(6)	1	0.006(2)

a) Fixed according to the nominal composition (see text for details).

b) Refined assuming that the total number of Sn1 and Sn11 atoms in the crystal structure is fixed as 6.

Table S2. Interatomic distances in the crystal structures of $Cu_{26-x}Fe_xV_2Sn_6S_{32}$.

$Cu_{25}Fe_1V_2Sn_6S_{32}$		$Cu_{24}Fe_2V_2Sn_6S_{32}$		$Cu_{23}Fe_3V_2Sn_6S_{32}$		$Cu_{22}Fe_4V_2Sn_6S_{32}$	
bond	**dist., Å**	**bond**	**dist., Å**	**bond**	**dist., Å**	**bond**	**dist., Å**
Cu1/Fe1-S2	2.2755(1)	Cu1/Fe1-S2	2.296(5)	Cu1/Fe1-S2	2.282(4)	Cu1/Fe1-S2	2.311(5)
Cu1/Fe1-S2	2.2755(1)	Cu1/Fe1-S2	2.296(5)	Cu1/Fe1-S2	2.282(4)	Cu1/Fe1-S2	2.311(5)
Cu1/Fe1-S2	2.2755(1)	Cu1/Fe1-S2	2.296(5)	Cu1/Fe1-S2	2.282(4)	Cu1/Fe1-S2	2.311(5)
Cu1/Fe1-S2	2.2755(1)	Cu1/Fe1-S2	2.296(5)	Cu1/Fe1-S2	2.282(4)	Cu1/Fe1-S2	2.311(5)
Cu2-S1	2.2697(1)	Cu2-S1	2.433(10)	Cu2-S1	2.318(8)	Cu2-S1	2.414(9)
Cu2-S2	2.3072(1)	Cu2-S2	2.286(9)	Cu2-S2	2.327(6)	Cu2-S2	2.279(6)
Cu2-S2	2.3072(1)	Cu2-S2	2.286(9)	Cu2-S2	2.327(6)	Cu2-S2	2.279(6)
Cu2-S2	2.3072(1)	Cu2-S2	2.286(9)	Cu2-S2	2.327(6)	Cu2-S2	2.279(6)
Cu3-S1	2.3577(1)	Cu3/V2-S1	2.320(7)	Cu3/V2-S1	2.346(6)	Cu3/V2-S1	2.342(8)
Cu3-S1	2.3577(1)	Cu3/V2-S1	2.320(7)	Cu3/V2-S1	2.346(6)	Cu3/V2-S1	2.342(8)
Cu3-S2	2.3539(1)	Cu3/V2-S2	2.340(5)	Cu3/V2-S2	2.349(4)	Cu3/V2-S2	2.352(5)
Cu3-S2	2.3539(1)	Cu3/V2-S2	2.340(5)	Cu3/V2-S2	2.349(4)	Cu3/V2-S2	2.352(5)
V1/Sn2-Cu3	2.7307(1)	V1-Cu3/V2	2.715(3)	V1/Cu4-Cu3/V2	2.720(2)	V1/Cu4-Cu3/V2	2.718(3)
V1/Sn2-Cu3	2.7307(1)	V1-Cu3/V2	2.715(3)	V1/Cu4-Cu3/V2	2.720(2)	V1/Cu4-Cu3/V2	2.718(3)
V1/Sn2-Cu3	2.7307(1)	V1-Cu3/V2	2.715(3)	V1/Cu4-Cu3/V2	2.720(2)	V1/Cu4-Cu3/V2	2.718(3)
V1/Sn2-Cu3	2.7307(1)	V1-Cu3/V2	2.715(3)	V1/Cu4-Cu3/V2	2.720(2)	V1/Cu4-Cu3/V2	2.718(3)
V1/Sn2-Cu3	2.7307(1)	V1-Cu3/V2	2.715(3)	V1/Cu4-Cu3/V2	2.720(2)	V1/Cu4-Cu3/V2	2.718(3)
V1/Sn2-Cu3	2.7307(1)	V1-Cu3/V2	2.715(3)	V1/Cu4-Cu3/V2	2.720(2)	V1/Cu4-Cu3/V2	2.718(3)
V1/Sn2-S1	2.3432(1)	V1-S1	2.251(6)	V1/Cu4-S1	2.325(6)	V1/Cu4-S1	2.317(8)
V1/Sn2-S1	2.3432(1)	V1-S1	2.251(6)	V1/Cu4-S1	2.325(6)	V1/Cu4-S1	2.317(8)
V1/Sn2-S1	2.3432(1)	V1-S1	2.251(6)	V1/Cu4-S1	2.325(6)	V1/Cu4-S1	2.317(8)
V1/Sn2-S1	2.3432(1)	V1-S1	2.251(6)	V1/Cu4-S1	2.325(6)	V1/Cu4-S1	2.317(8)
Sn1-S2	2.4029(1)	Sn1-S2	2.412(5)	Sn1-S2	2.397(4)	Sn1-S2	2.394(5)
Sn1-S2	2.4029(1)	Sn1-S2	2.412(5)	Sn1-S2	2.397(4)	Sn1-S2	2.394(5)
Sn1-S2	2.4029(1)	Sn1-S2	2.412(5)	Sn1-S2	2.397(4)	Sn1-S2	2.394(5)
Sn1-S2	2.4029(1)	Sn1-S2	2.412(5)	Sn1-S2	2.397(4)	Sn1-S2	2.394(5)
Sn11-S2	2.5161(1)						
Sn11-S2	2.3794(1)						
Sn11-S2	2.3708(1)						
Sn11-S2	2.3525(1)						
Sn11-Sn1	0.1147(1)						
Sn11-Sn1	0.1147(1)						
Sn11-Sn1	0.1147(1)						
Sn11-Sn1	0.1147(1)						

Table S3. Composition of the $Cu_{26-x}Fe_xV_2Sn_6S_{32}$ samples from crystal data and EDX spectroscopy.

Nominal composition	Composition from crystal data	Composition form EDXS data
$Cu_{25}FeV_2Sn_6S_{32}$	$Cu_{25}Fe_1V_{1,6(1)}Sn_{6,4(7)}S_{32}$	$Cu_{24,1(3)}Fe_{1,18(7)}V_{2,11(7)}Sn_{6,51(7)}S_{32,1(3)}$
$Cu_{24}Fe_2V_2Sn_6S_{32}$	$Cu_{23,3(1)}Fe_2V_{2,7(1)}Sn_6S_{32}$	$Cu_{23,5(3)}Fe_{2,2(1)}V_{2,1(1)}Sn_{6,4(1)}S_{31,8(3)}$
$Cu_{23}Fe_3V_2Sn_6S_{32}$	$Cu_{22,0(3)}Fe_{3,5(3)}V_{2,5(1)}Sn_6S_{32}$	$Cu_{22,3(4)}Fe_{3,3(1)}V_{2,0(1)}Sn_{6,4(2)}S_{32,0(1)}$
$Cu_{22}Fe_4V_2Sn_6S_{32}$	$Cu_{22,0(5)}Fe_{4,0(2)}V_{2,0(3)}Sn_6S_{32}$	$Cu_{21,5(3)}Fe_{4,3(3)}V_{1,9(2)}Sn_{6,3(2)}S_{32,0(2)}$

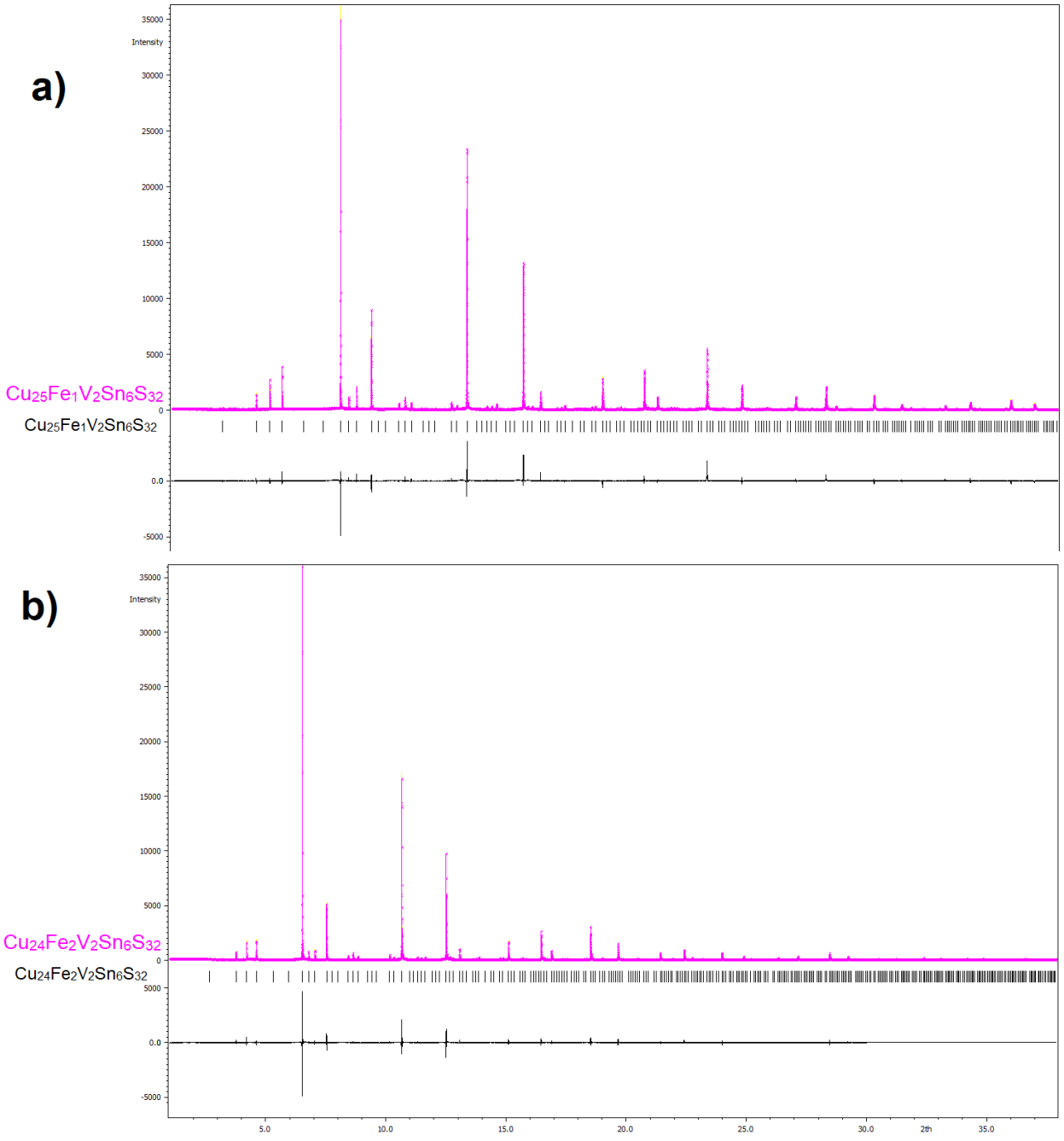
a)
Intensity
35000
30000
25000
20000
15000
10000
5000
0
Cu25Fe1V2Sn6S32
Cu25Fe1V2Sn6S32
0.0
-5000
b)
Intensity
35000
30000
25000
20000
15000
10000
5000
0
Cu24Fe2V2Sn6S32
Cu24Fe2V2Sn6S32
5000
0.0
-5000
5.0
10.0
15.0
20.0
25.0
30.0
2th
35.0

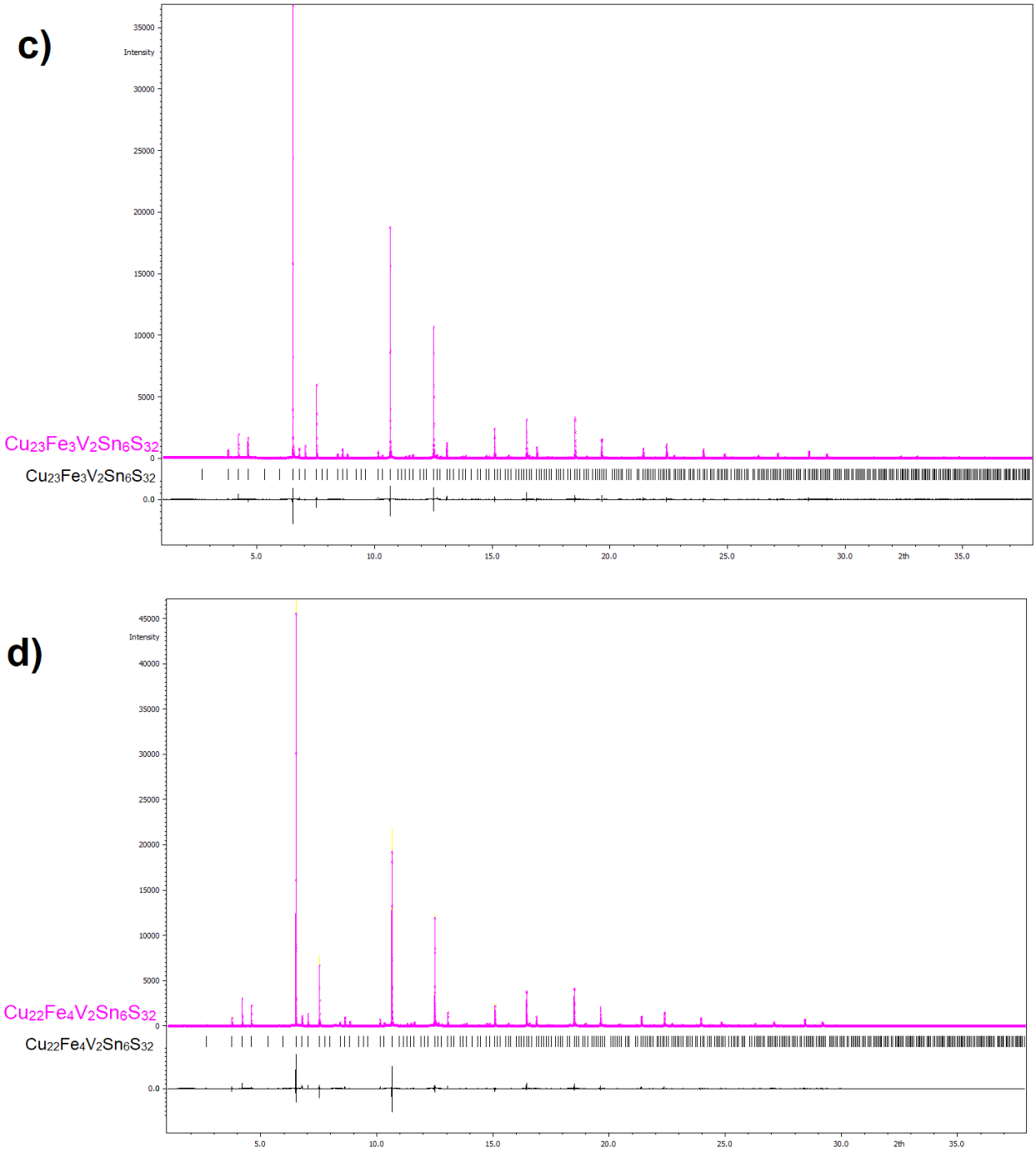

Figure S1. Rietveld refinement of the crystal structure of $Cu_{26-x}Fe_xV_2Sn_6S_{32}$ against synchrotron X-ray diffraction data for x = 1 (*a*); 2 (*b*); 3 (*c*); 4 (*d*). Shown are experimental and difference profiles and calculated peak positions.

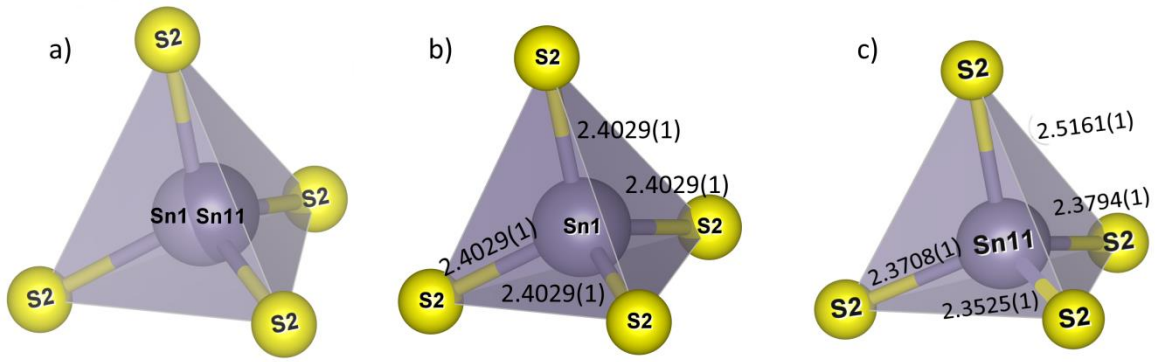

Figure S2. Local environment of Sn1 and Sn11 atoms in the crystal structure of $Cu_{25}Fe_1V_2Sn_6S_{32}$. Disposition of Sn1 and Sn11 atoms inside a tetrahedron (*a*) and Sn-S distances for Sn1 (*b*) and Sn11 (*c*) atoms. Only 1 of 4 possible Sn11 positions is shown for clarity.

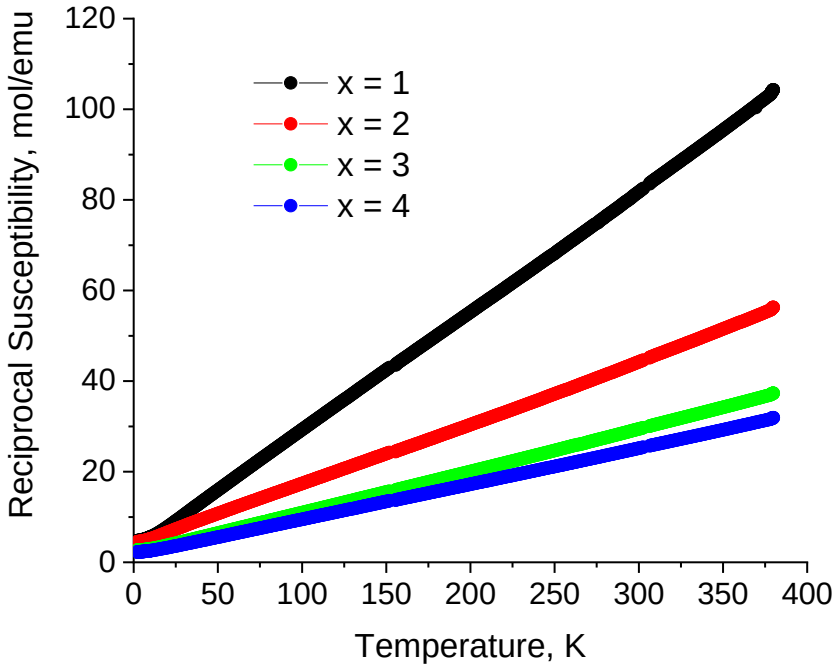

Figure S3. Reciprocal magnetic susceptibility as a function of temperature for $Cu_{26-x}Fe_xV_2Sn_6S_{32}$ in magnetic field of 5 T.

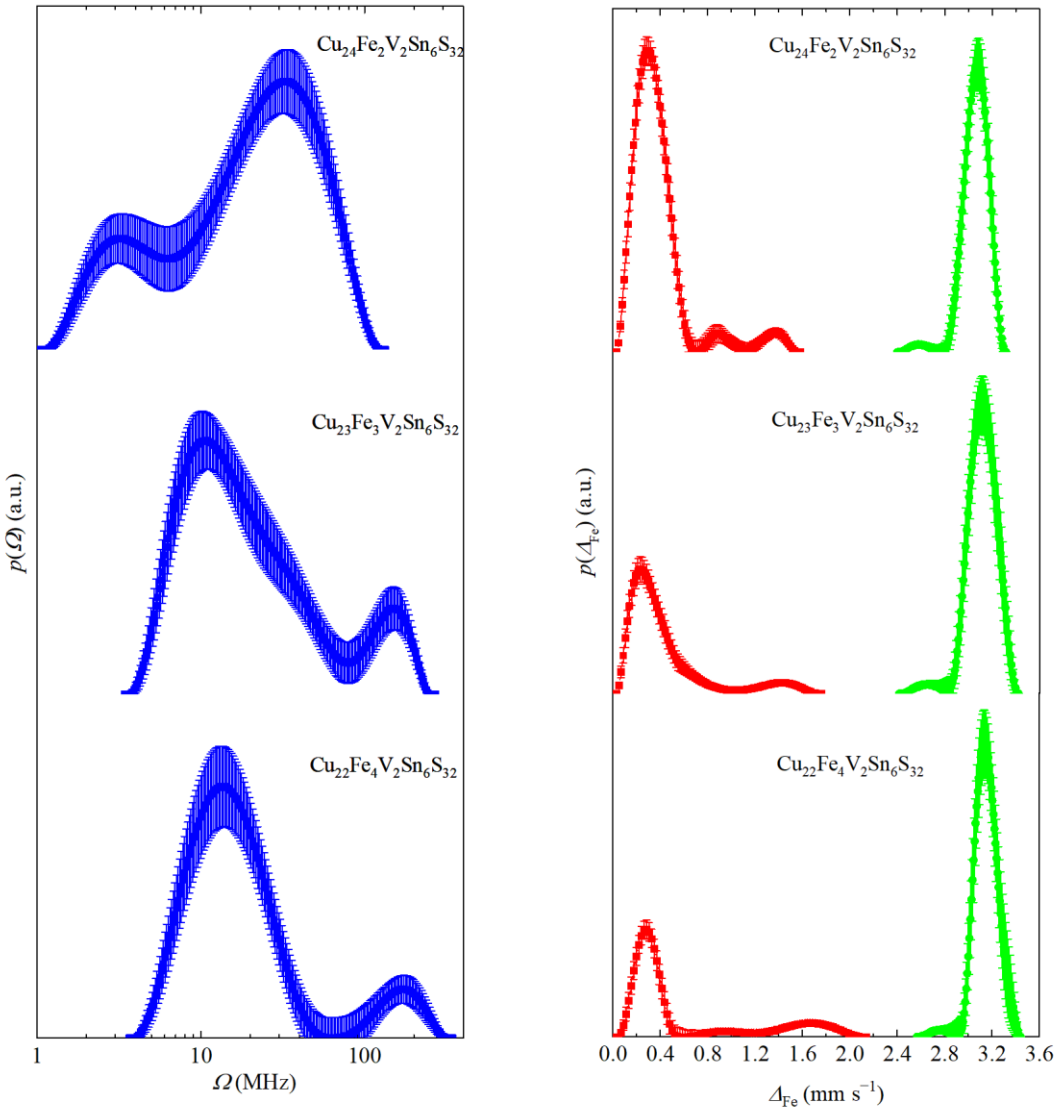

Figure S4. Relaxation frequencies distribution (left panel) of the "relax" component at 300 K; quadrupole splitting distribution (right panel) at 15 K.

Annex S1. Calculation of the lattice contribution to the EFG in Cu25FeV2Sn6S32.

The lattice contribution to the EFG at the Sn^{4+} sites was calculated using a monopole-point-dipole model [S1]. The monopole contribution (V_{ij}^{mon}) is given by

$$V_{ij}^{\text{mon}} = \sum_k Z_k (3x_{ik}x_{jk} - \delta_{ij}r_k^2)/r_k^5 , \qquad \text{(S1)}$$

where Z_k is the charge and x_{ik} (x_{jk}) are the Cartesian coordinates of the k-th ion with a distance r_k from the origin located at a given site, and δ_{ij} is the Kronecher index. The dipole contribution V_{ij}^{dip} is

$$V_{ij}^{\text{dip}} = \sum_k -3[(x_{ik}p_{ik})(5x_{ik}x_{jk} - \delta_{ij}r_k^2)/r_k^7 - (x_{ik}p_{ik} + x_{jk}p_{jk})/r_k^5] \qquad \text{(S2)}$$

where p_{ik} is the i-th component of the induced dipole moment on the k-th ion and the other symbols have the same meaning as in Eq. (S1). The components of the induced dipole moment are equal to

$$p_{ik} = \sum_i \alpha_{ij}^k E_j^k , \qquad \text{(S3)}$$

where α^k is the polarizability tensor of the *k*-th ion and E_j^k is the *j*-th component of the total electric field at the *k*-th ion. Since the induced dipole moments contribute to the electric field themselves, they have been calculated with a self-consistent iterative process. Due to the local symmetry at the sites of the $Cu^{2+/1+}$, $Fe^{3+/2+}$, Sn^{4+}, and V^{5+} cations and small ionic radii, a significant electric field E^k exists only at the sulfur sites in the $Cu_{25}FeV_2Sn_6S_{32}$ lattice. Thus, only the sulfur ions (α_S) contribute to V_{ij}^{dip}. The α_S value is not well known and was estimated from the best fit of the theoretical EFGs to the measured data. In our calculations, we used values of α_S in the range of 0 – 5.6 $Å^3$ [S2]. The lattice sums in Eq. (S1) and (S2) were calculated with the spherical boundary method in which the summation is carried out by considering the contributions from all lattice sites inside a given sphere radius (*r*) of 50 Å. The crystal pseudo cell was constructed from the crystal data reported in this paper and consists of 2×2×2 original unit cells where the tin atoms from the Sn11 site were randomly redistributed in accordance with its occupations. The quadrupole moment of the ^{119}Sn nucleus in the excited state, $Q = -0.109$ b [S3], and the Sternheimer antishielding factor for Sn^{4+} were not ever mentioned in the literature. Thus, we compare not the absolute values of the quadrupole splittings Δ for Sn1/2 and Sn11 but the $V_{ZZ}^{tot} = V_{ZZ}^{mon} + V_{ZZ}^{dip}$ values while $\Delta \approx (1-\gamma_\infty) eQV_{ZZ}^{tot}/2$ (γ_∞ is the Sternheimer factor for lattice contribution), with the exception of asymmetry parameter η for cubic crystals. Now, we can express the relation as

$$\frac{V_{ZZ}(Sn1/2)}{V_{ZZ}(Sn11)} = \frac{\Delta(Sn1/2)}{\Delta(Sn11)} \qquad \text{(S4)}$$

The sulfur dipole polarizability α_S has been estimated with a self-consistent iterative method from the fit of the calculated EFG components to the experimental values relation (S4) of quadrupole splitting. The best theoretical value at $\alpha_S = 2.8$ $Å^3$ of the relation (S4) is $\frac{V_{ZZ}(Sn1/2)}{V_{ZZ}(Sn11)} = 0.62$ and the experimental value $\frac{\Delta(Sn1/2)}{\Delta(Sn11)} \approx 0.68$.

Reference

1. Stadnik, Z.M. Electric field gradient calculations in rare-earth iron garnets // *J. Phys. Chem. Solids* **1984**, *45*, 311-318. https://doi.org/10.1016/0022-3697(84)90036-2.
2. Yatsenko, A.V. Analysis of the electronic dipole polarizability of ions in cubic oxides, fluorides, and sulfides of alkaline earth elements. *Crystallogr. Rep.* **2010**, *55*, 668–672. https://doi.org/10.1134/S106377451004022X.
3. Haas, H.; Menninger, M.; Andreasen, H.; Damgaard, S.; Grann, H.; Pedersen, F.T.; Petersen, J.W.; Weyer, G. EFG sign for Sn in Zn, Cd, and Sb. *Hyperfine Interact*. **1983**, *15/16*, 215-218. https://doi.org/10.1007/BF02159741